POLISH JOURNAL OF SOIL SCIENCE
VOL. LIII/1 2020 PL ISSN 0079-2985

DOI: 10.17951/pjss/2020.53.1.55

KHALID FATHI UBEID*, KHALED AHMED RAMADAN**

SOIL TYPES AND THEIR RELATIONS WITH RADON CONCENTRATION LEVELS IN MIDDLE GOVERNORATE OF GAZA STRIP, PALESTINE

Received: 21.01.2019
Accepted: 12.02.2020

Abstract. Determination of natural radioactivity has been carried out in surface and core agricultural soil samples collected from various sites in the Middle Governorate – Gaza Strip, Palestine. Mechanical and chemical analysis has been done to determine soil characteristics. Radon activity concentration measurements were carried out using solid state nuclear tracks detectors, Cr-39. The mechanical analysis results show that they belong to two classes, sandy loam and loamy sand. The sandy loam soil was observed in the eastern side of the study area, whereas the loamy sand was observed in western and middle parts. The radon concentration levels were higher in core samples and were proportionate to the soil depth. Also they were higher in sandy loam than loamy sand soil samples. The radon concentration levels had a positive correlation with fine grains (clay- to silt-size) of soil sample which translocated from upper to lower horizons of soil during its development. Additionally, there was a positive correlation with pH and water content, whereas a negative correlation was observed with organic matter and potassium contents. The positive correlation referred to a large specific surface of fine grains which were located in lower horizons of soil and were able to adsorb more water and consequently led to high radon concentration levels.

Keywords: grain-size distribution, radon, pollution, Gaza Strip, Palestine

* Department of Geology, Faculty of Science, Al Azhar University – Gaza, P.O. Box 1277, Gaza Strip, Palestine; corresponding author's e-mail: khubeid@hotmail.com

** Department of Physics, Faculty of Science, Al Azhar University – Gaza, P.O. Box 1277, Gaza Strip, Palestine.

1. INTRODUCTION

In addition to being the main source of continuous radiation exposure to human, soil acts as a medium of migration for transfer of radionuclides to the biological systems and hence, it is the basic indicator of radiological contamination in the environment. Moreover, the soil radioactivity is usually important for the purposes of establishing baseline data for future radiation impact assessment, radiation protection and exploration (Ramli *et al.* 2005). Various studies concerning radioactivity bound to soil were carried out by different researchers (e.g. Khatir *et al.* 1998, Tzortzis *et al.* 2003, Matiullah *et al*. 2004, Ramli *et al*. 2005, Veiga *et al*. 2006) and concerned various regions of the world. Most of these studies were concentrated on natural sources as the natural radiation is the largest contributor to the external dose provided to the world's population (UNSCEAR 2000). These dose rates vary from one place to another depending upon the concentration of natural radionuclides like ^{238}U, ^{226}Ra, ^{232}Th and ^{40}K present in soil. Data on natural radionuclides are still very scarce in Jordan and the previous studies are limited to specific regions, radionuclides and/or geological formation (e.g. El-Ghossain and Abu Saleh 2007, El-Ghossain and Abu Shammala 2012, Rasas *et al*. 2004, Ubeid and Ramadan 2017).

The aims of this work were the determination of radon concentration levels in surface and core agricultural soil samples collected from various soil types in different sites in the Middle Governorate of Gaza Strip, Palestine. Additionally, identification of the relationships of these concentration levels with soil characteristics and their contents was examined.

2. STUDY AREA

The Gaza Strip is located in the southwestern Palestine, at the southeastern coast of the Mediterranean Sea, between 34°2'E and 31°45'N (Fig. 1). It covers an area of approximately 365 km^2, has a length of 45 km along the coastal zone, and its width ranges from 5 to 8 km in the central and northern regions to the maximum of 12 km in the south. It is located in the transitional zone between a temperate Mediterranean climate in the west and north, and the arid climate of the Sinai Peninsula in the east and south. The temperature gradually changed throughout the year, reached its maximum during the summer (August), and its minimum during the winter (January). The average monthly maximum temperature ranges between 17.6°C for January and 29.4°C for August. The average of the monthly minimum temperature for January is about 9.6°C and 22.7°C for August. The mean annual rainfall is 335 mm per year, and the average annual evaporation is 1,300 mm. Gaza topography is defined by three ridges (locally termed *kurkar* ridges) and depressions, dry streambeds and shifting sand dunes

(Fig. 1). The ridges and depressions generally extend in the NE-SW direction, parallel to the coastline. The surface elevation ranges from mean sea level to about 110 m above mean sea level. The depressions, which contain alluvial deposits, are about 20–40 m above mean sea level. The Gaza Strip is divided into five governorates, the Northern Governorate, Gaza Governorate, the Middle Governorate, Khan Younis Governorate, and Rafah Governorate. The study area is located in the Middle Governorate (Fig. 1).

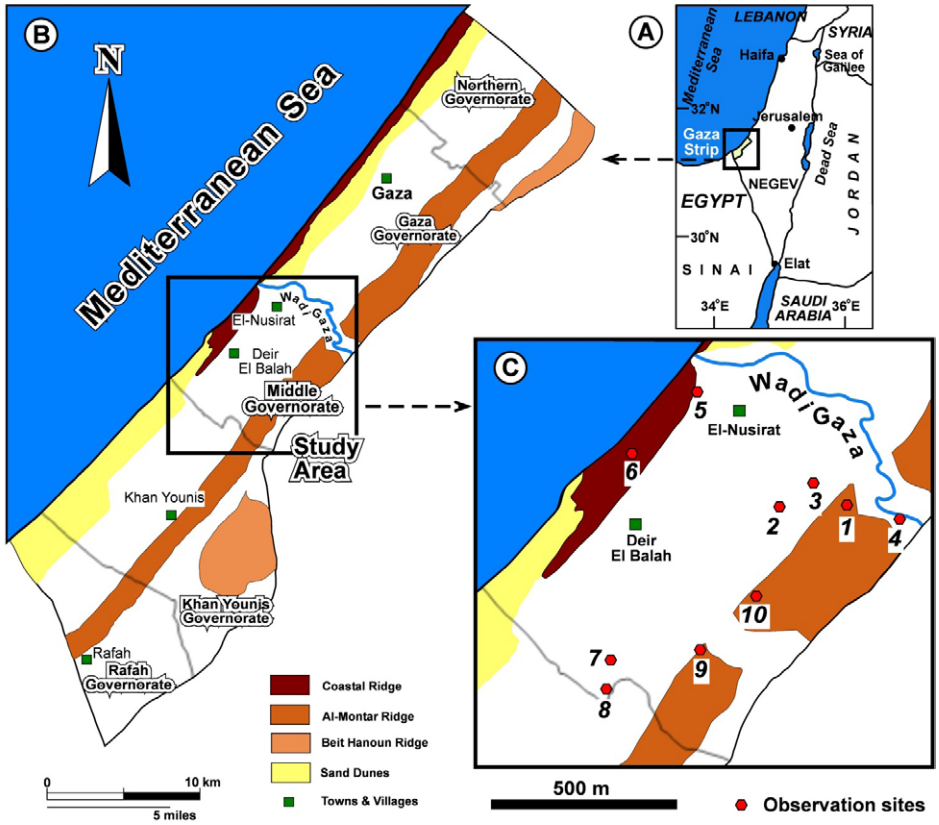

Fig. 1. Location of Gaza Strip showing the study sites

3. GEOLOGICAL OVERVIEW

Stratigraphically, these ridges belong to the Kurkar Group (Bartov *et al*. 1981). This group is of a Pliocene-Pleistocene age, and within this group three formations can be distinguished: Ahuzam Fm, Pleshet Fm, and Gaza Fm (Bartov and Arkin 1980, Frechen *et al*. 2004, Galili *et al*. 2007, Ubeid 2010, 2011). The *kurkar* ridges belonging to the Gaza Fm consist of calcareous sandstones (locally termed *kurkar*) alternated with brown reddish fine-grained deposits (locally

termed *hamra*) (Fig. 2) (Horowitz 1975, Abed and Al Weshahy 1999, Frechen *et al*. 2004, Ubeid 2010, 2011). In the southern part of the Gaza Strip these features tend to be covered by sand dunes. The soil in the Gaza Strip is mainly composed of three soil types: sandy soil, clayey soil, and loess soil (Ubeid 2011, 2013). The sandy soil was found along the coastline and middle parts of the Gaza Strip, in the form of sand dunes. The clayey soil is found along the northeastern part of the Gaza Strip. The loess soil is found around the Wadis.

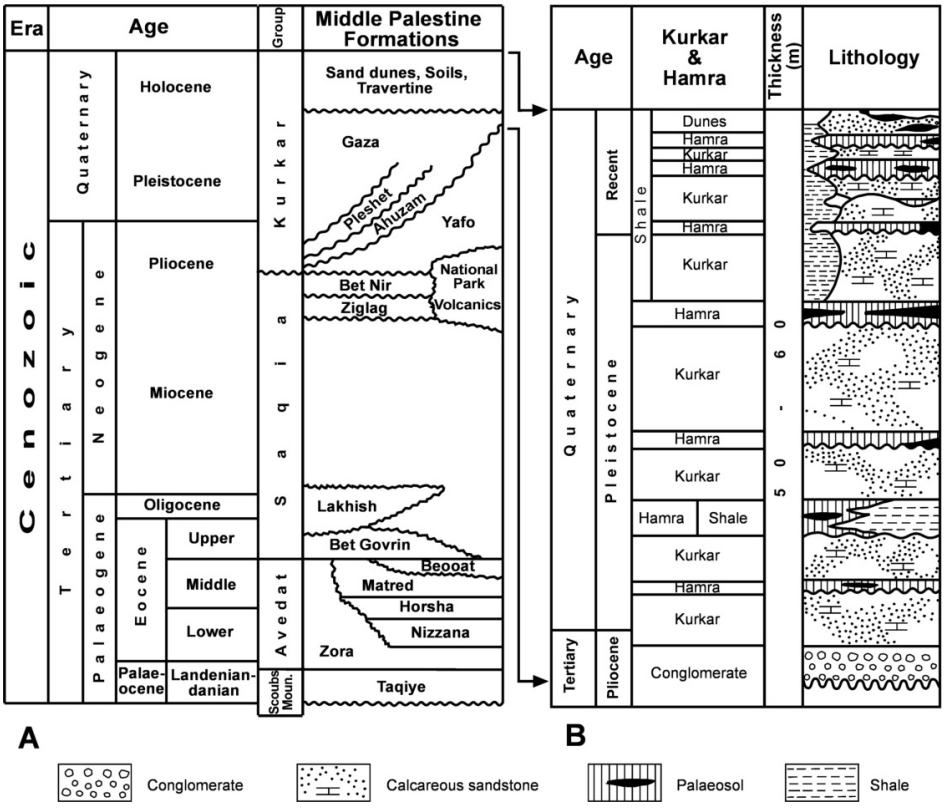

Fig. 2. Stratigraphy and sedimentology. (A) Stratigraphic succession of Tertiary and Quaternary in the central plain of Palestine; (B) lithology of Plio-Pleistocene Gaza Formation (Ubeid 2011)

4. METHODOLOGY

4.1. Field sampling

Classical field work was carried in the Middle Governorate of Gaza Strip. Ten observed sites were selected to collect samples from agriculture soils. The coordinates for each site were recorded by the GPS device (Table 1). At each

site, four fresh and represented samples were collected. One sample was taken from the surface, and the rest were core samples taken at a depth of 20, 40, and 60 cm. The samples were put in polyethylene bags and tightly closed. In addition to that, field observations for soil physical properties, time day sampling, temperature, and irrigation times were noted down. After field work the samples were directly transferred to the laboratory analysis.

Table 1. The coordinates of observation sites

Site no.	Sample no.	Location	Coordinates	
			N	E
1	1S	El-Bureij	31°25'40"	34°30'42.3"
	1C-20			
	1C-40			
	1C-60			
2	2S	El-Bureij	31°26'2.0"	34°24'35.4"
	2C-20			
	2C-40			
	2C-60			
3	3S	El-Bureij	31°26'19.6"	34°24'2.2"
4	4S	Wadi Gaza	31°25'51.7"	34°25'15.0"
	4C-20			
	4C-40			
	4C-60			
5	5S	El-Nusirat	31°27'25.8"	34°22'31.2"
6	6S	El-Zwaida	31°26'35.4"	34°21'38.5"
	6C-20			
	6C-40			
	6C-60			
7	7S	Dier El-Balah	31°23'46.3"	34°20'37.6"
	7C-20			
	7C-40			
	7C-60			
8-1	8S	Dier El-Balah	31°23'18.5"	34°20'34.4"
	8C-20			
	8C-40			
	8C-60			
8-2	8S-2	Dier El-Balah	31°23'18.5"	34°20'34.4"
9-1	9S	Dier El-Balah	31°24'4.1"	34°22'27.5"
	9C-20			
	9C-40			
	9C-60			
10	10S	El-Maghazi	31°24'48.2"	34°23'15.1"
	10C-20			
	10C-40			
	10C-60			

4.2. Laboratory analysis

4.2.1. Grain-size analysis

Primarily the coarse particles were removed from samples by the sieve (2,000 μm). Then, the samples were dried at 105°C for 24 hours in an oven. After drying, the sieving method was used for sandy soil samples by the sieve shaker to classify the particle sands of each sample, eight sieves were used (2,000, 1,180, 600, 425, 300, 212, 150, 63 μm). The initial weight of each sample was kept constant at 100 g, and the duration of shaking was about 15 minutes for each sample. The retained weight of sands in each sieve was determined separately. The results of grain-size analysis are generally expressed in terms of the percentage of the total weight of sample that passed through different sieves. For muddy soil samples, sedimentation analysis method (by using hydrometer and dispersive calgon) was done to separate the grain size. The data were processed using GRADISTAT software (Blott and Pye 2001) to obtain the grain-size distribution. The textural classes of the soil samples due to grain-size distribution results were defined by using the USDA soil texture triangle chart (Table 2).

Table 2. Grain-size distribution and textural classes of soil samples in the study area

Location	Sample no.	Depth (cm)	Clay (%)	Silt (%)	Sand (%)	Soil texture class
1	1S	0	2	25	73	Sandy loam
	1C/1	20	2	28	70	
	1C/2	40	2	28	70	
	1C3	60	2	41	57	
2	2S	0	1	25	74	Sandy loam
	2C/1	20	2	32	66	
	2C/2	40	1	49	66	
	2C/3	60	2	38	60	
3	3S	0	1	33	66	Sandy loam
4	4S	0	4	32	64	Sandy loam
	4C/1	20	2	24	74	
	4C/2	40	1	43	56	
	4C/3	60	1	25	74	
5	5S	0	4	10	86	Loamy sand
6	6S	0	2	20	78	Loamy sand
	6C/1	20	2	28	70	
	6C/2	40	2	36	62	
	6C/3	60	2	24	74	
7	7S	0	3	32	65	Loamy sand
	7C/1	20	1	25	74	
	7C/2	40	2	28	70	
	7C/3	60	1	17	82	

8/1	8S/1	0	4	24	72	Loamy sand
	8C/1	20	1	22	77	
	8C/2	40	8	8	84	
	8C/3	60	8	12	80	
8/2	8S/2	0	2	8	90	Loamy sand
9/1	9S/1	0	1	25	74	Loamy sand
	9C/1	20	6	26	68	
	9C/2	40	2	20	78	
	9C/3	60	4	34	62	
10	10S	0	6	22	72	Sandy loam
	10C/1	20	2	28	70	
	10C/2	40	2	44	54	
	10C/3	60	2	34	64	

4.2.2. Chemical analysis

Chemical analysis for pH, water contents (WC), organic matter contents (OMC), and potassium contents of soil samples was done in laboratories of Geology Department in Al Azhar University – Gaza. For pH determination, around 20 gm of dry soil was transferred into a 100 ml beaker, and 40 ml distilled water was added and stirred well with a glass rod. This was allowed for half an hour with intermittent stirring. Then the pH meter 3310 electrode (Fenway UK) was used to determine pH value. The water contents were determined by drying soil samples in an oven up to 105°C for 24 hours. The water contents were measured by the weight difference between the wet and dry sample. Based on ASTM D2974 Standard Test Methods for Moisture, Ash, and Organic Matter of Peat and Other Organic Soils, the organic matter contents in the soil samples were determined. In this method the samples were heated in a muffle furnace up to 440°C. The organic matter was measured by the weight difference between the sample before and after drying.

For potassium determination, around 5 gm of dried soil was diluted in the solution of distilled water (100 ml) with sodium bicarbonate (0.5 gm). The solution was shaken for 30 min. After filtering the solution through 42 filter paper, the potassium contents were determined by the spectroscopy method, using a flame photometer instrument.

4.2.3. Radon concentration measurement

The sealed-cup technique and CR-39 detectors were used for measuring the radium content and radon exhalation rate from the soil samples (Fig. 3). 300 ml of dried soil samples are put in container (3L), CR-39 films are pasted on the lower side of cover, after tightening the cover, the containers were sealed with adhesive tape to minimize the leakage and left for 80 days so that the plastic tracks

detectors (CR-39) can record enough alpha particles as a result of radon disintegrations. At the end of the exposure time, CR-39 films were etched, using a 6M solution of NaOH, at a temperature of 70°C, for about 5 hours. The detectors were washed with distilled water and left to dry. Each detector was counted visually using an optical microscope through the area within 3 mm^2 in 4 distinct regions, and the average number of tracks/mm^2 was determined from the measured average track densities on the CR-39, with detector efficiency of around 12.3 tracks cm^{-2} $month^{-1}$ per Bq/m^3. Radon calculations in this study were carried out using the following equations:

$$E = \frac{k\rho}{A}\left[\frac{\lambda V}{T_{eff}}\right], \quad C_{Rn} = k\frac{\rho}{T_{eff}}, \quad C_{Ra} = k\frac{\rho V}{MT_{eff}}$$

Where:

E is radon exhalation rate (Bq m^{-2} h^{-1})
C_{Rn} is the radon concentration (Bq/m^3)
C_{Ra} is the effective radium content (Bq/kg)
ρ is the track density (tracks/cm^2)
k is the detector sensitivity (Bq m^{-3}/tracks cm^{-2} h^{-1})
λ is the decay constant ($\lambda = 7.56 \times 10^{-3}$ h^{-1})
V is the void volume of the container (cm^3)
A is the area of the sample (cm^2)
M is the mass of the sample (kg) (Baykara and Dogru 2006, Baykara *et al*. 2005, Sroor *et al*. 2001).

The effective dose for one year radon exposure is calculated using the relation $AED = \varepsilon f_{Rn} T C_{Rn}$

Where:

f_{Rn} is the conversion factor = 9 nSv/(Bq h/m^3)
T is the time spent indoors per year = 7,000 hours
ϵ is the equilibrium factor (= 0.4)
C_{Rn} is the radon concentration (Guo and Cheng 2005).

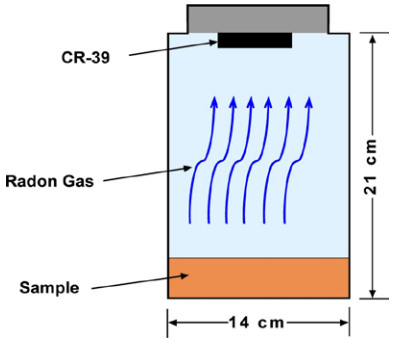

Fig. 3. Experimental setup for the measurement of radon exhalation rate

5. RESULTS AND DISCUSSION

5.1. Soil characteristics

The results of grain-size analysis are presented in Table 2. It shows that the soil samples in the study area can be divided into two classes. The first class was sandy loam, which included samples 1, 2, 3, 4, and 10. This class was located in

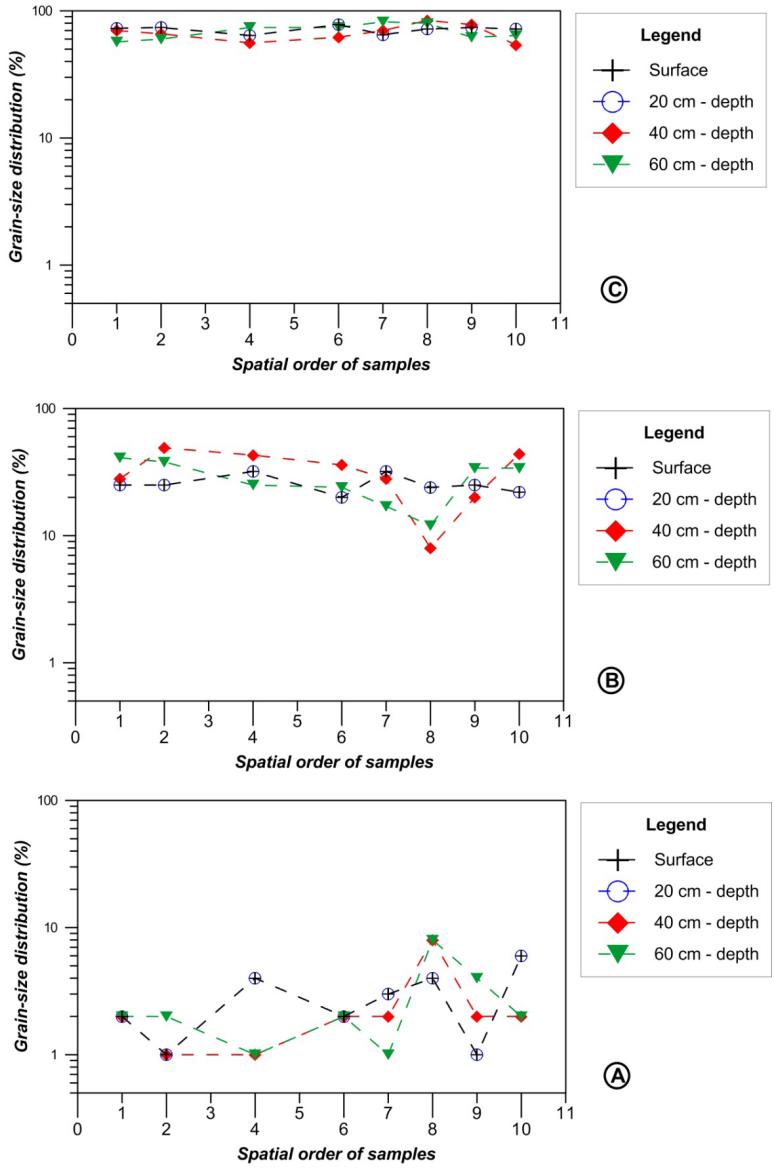

Fig. 4. Grain-size distribution in surface and cores samples of studied sites. (A) clay-size distribution, (B) silt-size distribution, (C) sand-size distribution

the eastern side of the study area. The second class was loamy sand, and it included samples 5, 6, 7, 8, and 9. This class was mostly located in the western and middle sides, where the sand dunes were dominant. Generally, this part of the study area characterized by dominant fine- to medium grain-size of sand (Ubeid and Albatta 2014). The results of grain-size distribution for the surface sample (1S to 4S and 10S) in the study area show that the fine-grained sediments (clay- to silt-size) in sandy loam class ranges from 26 to 34%, and the sand-grained ranges from 64 to 74%, whereas in the core samples (5C to 9C) of sandy loam class the clay- to silt-grained ranges from 26 to 50%, and the sand-grained from 54 to 74%. On the other side, the fine-grained (clay- to silt-size) in surface samples (1S to 4S and 10S) of loamy sand class ranges from 10 to 35%, and the sand-grained from 62 to 90%, whereas the clay- to silt-grained in the core samples (5C to 9C) of loamy sand class ranges from 16 to 38%, and the sand-grained from 62 to 84% (Fig. 4).

Overall, the results of grain-size analysis show that the fine-grained (clay- to silt-size) sediments were found with high percentage in samples of sandy loam class which were located in eastern side of the study area. More precisely, the highest percentage was observed in the core samples in the same soil class. The lowest percentage of the fine-grained were observed in surface samples, especially in loamy sand classes which were located in western and middle parts of the study area. Table 3 depicted the results of chemical analysis. The results show that the high values of pH and water content (WC) in soil samples were observed in the core samples. The highest value of pH was about 8.69 in a sandy loam class, while the highest value – about 8.49 – in loamy sand. The WC recorded the highest value in a sandy loam class with about 15.91%, while the highest value was about 13.12% in a loamy sand soil class (Figs. 5 and 6). However, the correlation between the grain-size of soil samples and their pH and water contents were characterized by an inverse relationship. This fact indicates that the pH and WC values increase with decreasing the grain-size, due to large specific area of fine-grained which were able to adsorb more water.

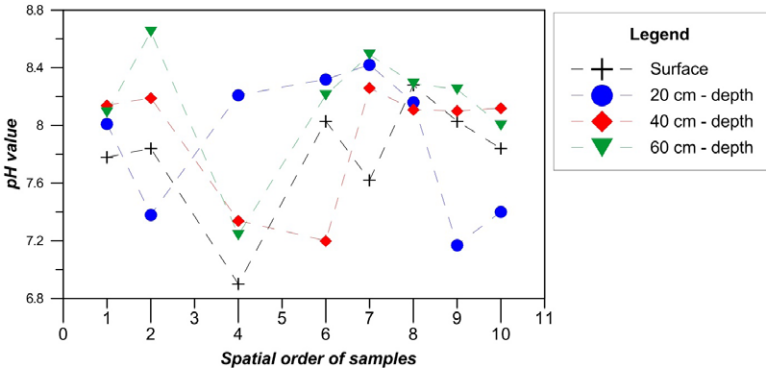

Fig. 5. pH values in surface and core samples of the studied sites

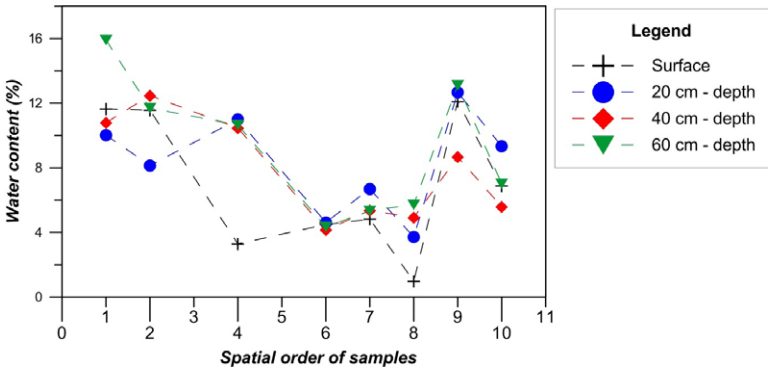

Fig. 6. Water contents in soil samples of the study area

The organic matter and potassium contents in soil samples had the highest values in surface samples (S) and in uppermost core samples (C/1) in studied sites (Table 3, Figs. 7 and 8). The value of organic matter contents (OMC) in surface and uppermost core samples varied from 0.55 to 3.82%. Additionally, the potassium values in S and C/1 samples varied from 20.8 to 64.8 mg/kg, where the nature of soil is characterized by the presence of high contents of organic matter in uppermost soil called "A-Horizon", and the decrease with the increasing depth of soil. Generally, there is a good positive correlation between the fertilizers or OMC and potassium contents.

Table 3. Radon activity concentrations levels, pH, water contents (WC), organic matter contents (OMC), and potassium contents (K) in soil samples of the study area. E = Radon Exhalation Rate, C_{Rn} = radon concentration, C_{Ra} = effective radium Content, and AED = annual effective dose

Location	Sample no.	Depth (cm)	pH	WC (%)	OMC (%)	K (mg/kg)	E (Bq/m^2 h)	C_{Rn} (Bq/m^3)	C_{Ra} (Bq/kg)	AED (mSv/y)
1	1S	0	7.78	11.65	1.48	46.2	0.52	518.2	3.35	13.1
	1C/1	20	8.01	10.02	2.74	30.0	0.31	302.9	1.94	7.6
	1C/2	40	8.14	10.79	1.44	20.8	1.35	1336.9	9.09	33.7
	1C3	60	8.09	15.91	0.78	25.4	1.74	1722.4	12.24	43.4
2	2S	0	7.84	11.56	2.35	42.0	1.41	1402.0	8.30	35.3
	2C/1	20	7.38	8.14	1.28	37.0	1.50	1492.1	8.76	37.6
	2C/2	40	8.19	12.47	1.88	27.8	2.39	2373.3	15.15	59.8
	2C/3	60	8.65	11.70	1.17	27.8	1.82	1802.5	11.64	45.4
3	3S	0	7.85	2.79	2.52	53.2	1.86	1842.6	11.99	46.4
4	4S	0	6.90	3.29	2.57	62.6	2.29	2273.2	15.42	57.3
	4C/1	20	8.21	10.99	1.18	20.8	2.77	2743.8	17.72	69.1
	4C/2	40	7.34	10.46	1.22	16.0	2.24	2223.1	14.68	56.0
	4C/3	60	7.24	10.65	1.64	25.4	1.48	1472.1	10.46	37.1
5	5S	0	7.96	2.10	1.24	34.6	1.13	1121.6	6.47	28.3

Location	Sample no.	Depth (cm)	pH	WC (%)	OMC (%)	K (mg/kg)	E (Bq/m^2 h)	C_{Rn} (Bq/m^3)	C_{Ra} (Bq/kg)	AED (mSv/y)
6	6S	0	8.03	4.49	0.93	44.0	0.56	550.8	3.49	13.9
	6C/1	20	8.32	4.62	0.73	20.8	0.43	425.6	2.56	10.7
	6C/2	40	7.20	4.15	0.63	27.8	0.46	455.6	2.62	11.5
	6C/3	60	8.21	4.34	0.49	20.8	0.73	721.0	4.06	18.2
7	7S	0	7.62	4.82	1.93	64.8	0.18	182.8	1.18	4.6
	7C/1	20	8.42	6.69	3.19	27.8	1.56	1542.1	10.62	38.9
	7C/2	40	8.26	5.36	1.02	20.8	2.06	2042.8	12.86	51.5
	7C/3	60	8.49	5.34	0.67	25.4	1.02	1011.4	6.35	25.5
8/1	8S/1	0	8.28	0.97	0.58	32.4	0.50	495.7	3.02	12.5
	8C/1	20	8.16	3.72	0.55	25.4	0.43	430.6	2.67	10.9
	8C/2	40	8.11	4.92	0.69	25.4	1.62	1602.2	10.28	40.4
	8C/3	60	8.29	5.72	1.10	27.8	0.73	721.0	4.50	18.2
8/2	8S/2	0	8.28	11.81	1.33	53.4	0.86	851.2	4.81	21.4
9/1	9S/1	0	8.03	12.11	1.27	25.4	1.61	1592.2	11.25	40.1
	9C/1	20	7.17	12.67	0.56	20.8	1.42	1412.0	8.11	35.6
	9C/2	40	8.10	8.67	3.39	20.8	1.91	1892.6	10.54	47.7
	9C/3	60	8.25	13.12	1.18	27.8	2.42	2398.3	15.45	60.4
10	10S	0	7.84	6.89	3.82	48.6	2.08	2062.9	17.57	52.0
	10C/1	20	7.40	9.34	1.87	50.0	2.80	2773.9	20.86	69.9
	10C/2	40	8.12	5.59	1.89	44.0	1.92	1902.7	13.52	47.9
	10C/3	60	8.00	7.02	2.87	39.4	2.46	2443.4	16.58	61.6

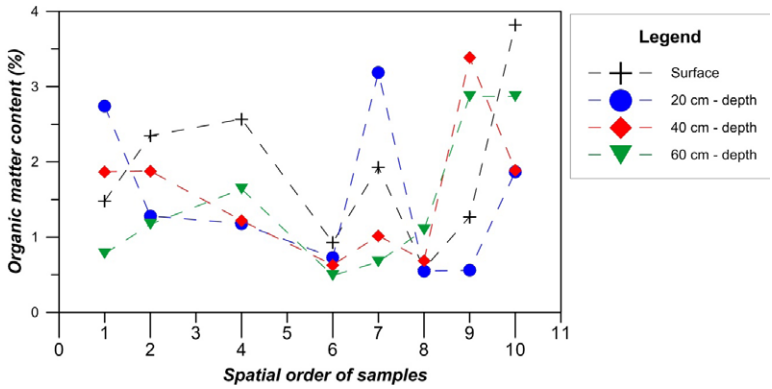

Fig. 7. Organic matter contents in soil samples of the study area

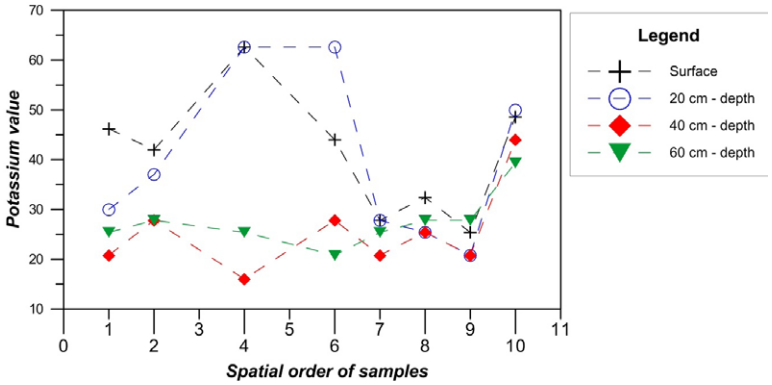

Fig. 8. Potassium values in soil samples of the study area

5.2. The radioactivity concentrations

The results of radioactivity concentrations of radon in soil samples of the study area are presented in Table 3, Table 4, and Fig. 9. It shows that the radioactivity levels of radon in the surface sandy loam soil class (1S to 4S and 10S) range from 3.35 to 17.57 Bq/kg, and from 1.94 to 20.86 Bq/kg in core samples (1C to 4C and 10C), whereas the levels of radioactivity concentrations in the surface loamy sand soil class (5S to 9S) range from 1.18 to 11.25 Bq/kg, and from 2.56 to 15.45 Bq/kg in core samples (5C to 9C). Fig. 10 shows that the linear correlation coefficient between radon concentrations and effective radium content was 0.98. This result shows the much stronger linear correlation between radon concentration and effective radium content. The linear correlation coefficient between the radon exhalation rate and effective radium concentration was 0.99 (Fig. 11).

Table 4. Statistical descriptive of radon activity concentrations levels, pH, water contents (WC), organic matter contents (OMC), and potassium contents (K) in soil samples of the study area. E = Radon Exhalation Rate, C_{Rn} = radon concentration, C_{Ra} = effective radium Content, and AED = annual effective dose

Location		pH	WC (%)	OMC (%)	K (mg/kg)	E (Bq/m^2h)	C_{Rn} (Bq/m^3)	C_{Ra} (Bq/Kg)	AED (mSv/y)
1	Min.	7.78	10.02	1.44	20.80	0.31	302.90	1.94	7.60
	Max.	8.09	15.91	2.74	46.20	1.74	1722.40	12.24	43.40
	Mean	8.01	12.09	1.61	30.60	0.98	970.10	6.66	24.45
	St. Dev.	0.16	2.63	0.82	11.06	0.68	670.79	4.84	16.91
2	Min.	7.38	8.14	1.17	27.80	1.41	1402.00	8.30	35.30
	Max.	8.65	12.47	2.35	42.00	2.39	2373.30	15.15	59.80
	Mean	8.02	10.97	1.67	33.65	1.78	1767.48	10.96	44.53
	St. Dev.	0.54	1.93	0.55	7.06	0.44	438.81	3.16	11.06

Location		pH	WC (%)	OMC (%)	K (mg/kg)	E (Bq/m^2h)	C_{Rn} (Bq/m^3)	C_{Ra} (Bq/Kg)	AED (mSv/y)
4	Min.	6.90	3.29	1.18	16.00	1.48	1472.10	10.46	37.10
	Max.	8.21	10.99	2.57	62.60	2.77	2743.80	17.72	69.10
	Mean	7.42	8.85	1.65	31.20	2.20	2178.05	14.57	54.88
	St. Dev.	0.56	4.01	0.65	21.28	0.53	525.84	3.03	13.23
6	Min.	7.20	4.15	0.49	20.80	0.43	425.60	2.56	10.70
	Max.	8.32	4.62	0.93	44.00	0.73	721.00	4.06	18.20
	Mean	7.94	4.40	0.70	28.35	0.545	538.25	3.1825	13.575
	St. Dev.	0.51	0.20	0.19	10.94	0.14	133.01	0.72	3.37
7	Min.	7.62	4.82	1.02	20.80	0.18	182.80	1.18	4.60
	Max.	8.49	6.69	3.19	27.80	2.06	2042.80	12.86	38.90
	Mean	8.20	5.56	1.70	34.70	1.21	1194.78	7.75	30.13
	St. Dev.	0.40	0.80	1.12	20.28	0.80	795.30	5.15	20.06
8	Min.	8.11	0.97	0.55	25.4	0.43	430.60	2.67	10.90
	Max.	8.29	5.72	1.10	32.40	1.62	1602.20	10.28	40.40
	Mean	8.21	3.83	0.73	27.75	0.82	812.38	5.12	20.50
	St. Dev.	0.02	2.22	0.27	3.43	0.58	569.22	3.71	14.34
9	Min.	7.17	8.67	0.56	20.80	1.42	1412.00	8.11	35.60
	Max.	8.25	13.12	3.39	27.80	2.42	2398.30	15.45	60.40
	Mean	7.89	11.64	1.60	23.70	1.84	1823.78	11.34	45.95
	St. Dev.	0.49	2.02	1.23	3.49	0.44	431.28	3.05	10.85
10	Min.	7.4	5.59	1.87	39.40	1.92	1902.70	13.52	47.90
	Max.	8.12	9.34	3.82	50.00	2.46	2773.90	20.86	69.9
	Mean	7.84	7.21	2.61	45.50	2.315	2295.73	17.1325	57.85
	St. Dev.	0.31	1.56	0.93	4.81	0.39	391.21	3.02	9.87

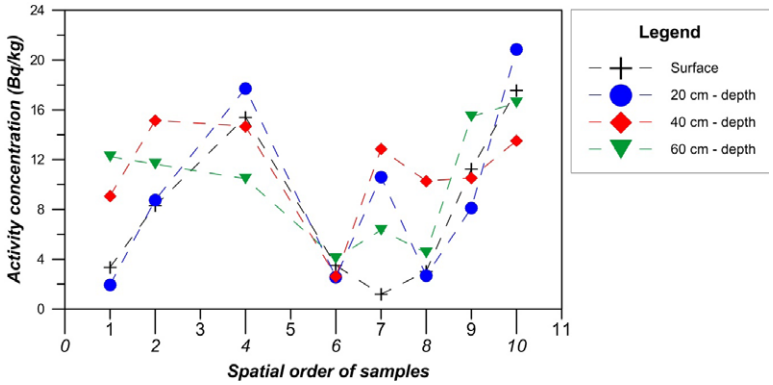

Fig. 9. Activity concentration levels in soil samples of the study area

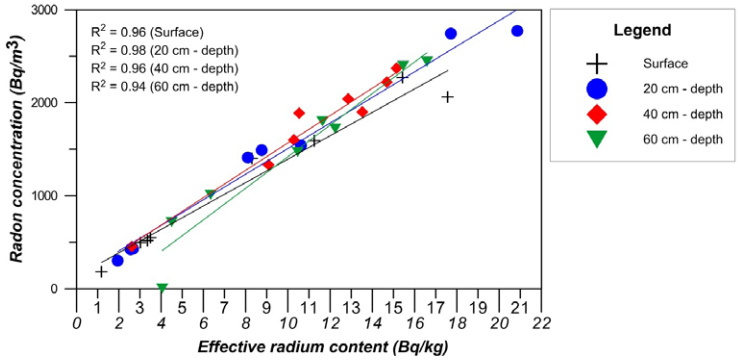

Fig. 10. Relationship between effective radium content (C_{Ra}) and radon concentration (C_{Rn})

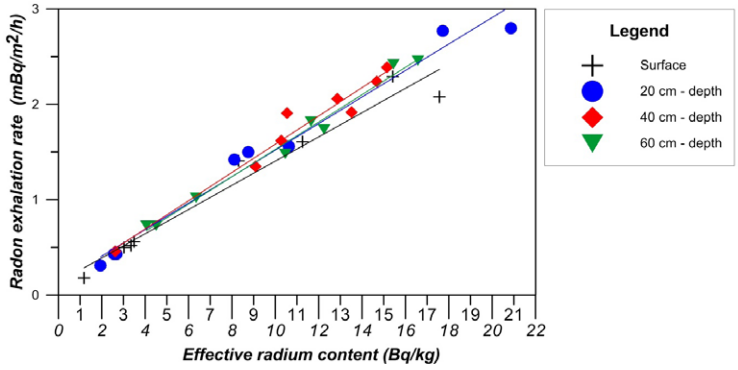

Fig. 11. Relationship between effective radium content (C_{Ra}) and radon exhalation rate (E)

Generally, the results of radioactivity concentration in the study area show that the concentration levels in core samples were higher comparing with surface samples. Moreover, the concentration levels were higher in both surface and core samples of sandy loam soil class which were located in eastern side of the study area comparing with surface and core samples of loamy sand soil class located in western and middle parts of the study area.

Overall, the radioactivity concentration levels had good correlation with fine-grained sediments. They were higher with the fine-grained sediments, which normally accumulated below the surface horizon called "B-Horizon". Consequently, the large specific surface of fine-grained sediments (clay- to silt-size) increased the adsorption of radon as well as the water contents and pH comparing with coarse-grained (sands) that accumulated in the soil surface. To sum up, the radioactivity concentration levels were directly proportional to these three factors as depicted in Figs. 9, 4, and 12. The obtained values are generally compatible with the literature (Shweikani *et al*. 1995, Abumurad *et al*. 1997, Jonsson 2001, Khayrat *et al*. 2001, Baixeras *et al*. 2001, Al-Jundi *et al*. 2003, Fujiyoshi and Sawamura 2004, Schubert *et al*. 2005, Shafi-ur-Rehman *et al*. 2006, Faheem and Matiullah 2008, Duggal *et al*. 2015, Nelson and Rittenour 2015).

On the other hand, the radioactivity concentrations were inversely proportional to organic matter and potassium contents in the soil sample, which were characterized by high levels in the surface and uppermost soil samples which were characterized by the accumulation of coarse-grained (sands) (Fig. 4). This suggests that fine-grained sediments were the main factor controlling the high levels of radioactivity, pH, and water contents.

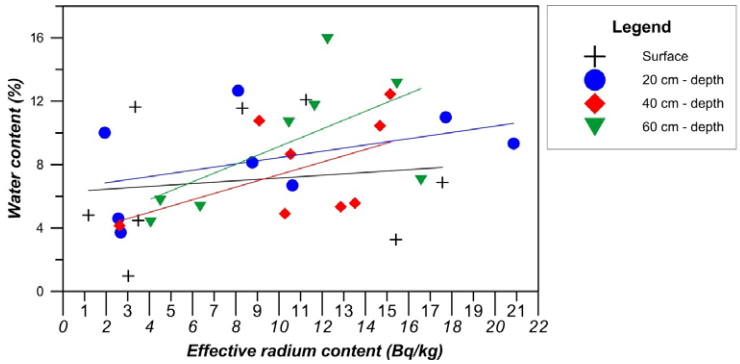

Fig. 12. Relationship between the radon activity and water content values in surface and core samples

CONCLUSIONS

Thirty-five core samples were collected from ten sites in the Middle Governorate of Gaza Strip. These samples were analyzed for soil characteristics and radon exhalations. Mechanical and chemical analyses were carried out to determine soil characteristics, and the solid state nuclear tracks detector (Cr-39) was used for measuring radon activity concentrations. The soil samples in all observation sites were grouped into two classes, sandy loam and loamy sand. The sandy loam soil class which was dominated by fine grains (clay- to silt-size) was observed in the eastern side of the study area, while the loamy sand soil class was dominated by coarse grains (very fine- to fine sand-size), which was observed in western and middle parts of the study area. The grain-size distribution of soil samples shows that there was an inverse relationship between the grain-size and the depth of core samples.

The results of measuring samples show that the radon concentration levels were higher in core samples comparing with the surface sample of the study area. Also the levels were higher in the sandy loam class when compared with the loamy sand soil class. The average radon concentration levels in surface sandy loam samples range from 3.35 to 17.57 Bq/kg, and from 1.94 to 20.86 Bq/kg in core samples, while the average levels in surface loamy sand sample range from 1.18 to 11.25 Bq/kg, and from 2.56 to 15.45 Bq/kg in core samples. The radon concentration levels had a positive correlation with fine-grain (clay-

to silt-size) sediments, pH, and water contents, and a negative correlation with organic matter and potassium contents. The positive correlation was referred to a large specific surface of fine grains which were able to adsorb more radon and water, whereas the negative correlation referred to the organic matter contents which had a good correlation with potassium naturally found in the surface of soil which lacks the finer fraction of the sediments, consequently, the ability of adsorption of radon going down.

REFERENCES

[1] Abed, A., Al Weshahy, S., 1999. *Geology of Palestine*. Palestinian Hydrogeological Group, Palestine, Jerusalem, 461 pp.

[2] Abumurad, K.M., Atrallah, M., Kullab, M.K., Ismail, A., 1997. *Determination of radon soil concentration levels in the governorate of Irbid, Jordan*. Radiation Measurements, 28: 585–588.

[3] Al-Jundi, J., Al-Bataina, B.A., Abu-Rukah, Y., Shehadeh, H.M., 2003. *Natural radioactivity concentrations in soil samples along the Amman Aqaba Highway, Jordan*. Radiation Measurements, 36: 555–560.

[4] Baixeras, C., Erlandsson, B., Font, LI, Jonsson, G., 2001. *Radon emanation from soil samples*. Radiation Measurements, 34: 441–443.

[5] Bartov, Y., Arkin, Y., 1980. *Regional stratigraphy of Israel. A guide to geological mapping*. Geological Survey of Israel. Current Research, 38–41.

[6] Bartov, Y., Arkin, Y., Lewy, Z., Mimran, Y., 1981. *Regional stratigraphy of Israel: A guide to geological mapping*. Geological Survey of Israel, Stratigraphic Chart.

[7] Baykara, O., Dogrua, M., Inceozb, M., Aksoyb, E., 2005. *Measurements of radon emanation from soil samples in triple-junction of North and East Anatolian active faults systems in Turkey*. Radiation Measurement, 39: 209–212.

[8] Baykara, O., Dogru, M., 2006. *Measurements of radon and uranium concentration in water and soil samples from East Anatolian Active Fault systems, Turkey*. Radiation Measurement, 41: 362–367.

[9] Blott, S.J., Pye, K., 2001. *Gradistat: A grain size distribution and statistics package for analysis of unconsolidated sediments*. Earth Surface Processes and Landforms, 26: 1237–1248.

[10] Duggal, V., Mehera, R., Rani, A., 2015. *Study of radium and radon exhalation rate in soil samples from areas of Northern Rajasthan*. Journal of the Geological Society of India, 86: 331–336.

[11] El-Ghossain, M.O., Abu Saleh, R.M., 2007. *Radiation measurements in soil in the middle of Gaza-Strip using different type of detectors.* IUG Journal of Natural Studies, 15: 23–37.

[12] El-Ghossain, M.O., Abu Shammala, A.A., 2012. *Radioactivity measurements in tap water in Gaza Strip (Al-Naser Area)*. Journal of the Association of Arab Universities for Basic and Applied Sciences, 11: 2–26.

[13] Faheem, M., Matiullah, 2008. *Radon exhalation and its dependence on moisture content from samples of soil and building materials*. Radiation Measurements, 43: 1458–1462.

[14] Frechen, M., Neber, A., Tsatskin, A., Boenigk, W., Ronen, A., 2004. *Chronology of Pleistocene sedimentary cycles in the Carmel coastal plain of Israel*. Quaternary International, 121: 41–52.

[15] Fujiyoshi, R., Sawamura, S., 2004. *Mesoscale variability of vertical profiles of environmental radionuclides (^{40}K, ^{226}Ra, ^{210}Pb and ^{137}Cs) in temperate forest soils in Germany*. Science of the Total Environment, 320: 177–188.

[16] Galili, E., Zviely, D., Ranon, A., Mienis, H.K., 2007. *Beach deposits of MIS 5e high sea stand as indicators for tectonic stability of the Carmel coastal plain, Israel*. Quaternary Science Reviews, 26: 2544–2557.

[17] Guo, Q., Cheng, J., 2005. *Indoor thoron and radon concentrations in Zhuhai, China*. Journal of Nuclear Science and Technology, 42: 588–591.
[18] Horowitz, A., 1975. *The quaternary stratigraphy and paleogeography of Israel*. Paléorient, 3: 47–100.
[19] Jonsson, G., 2001. *Soil radon depth dependence*. Radiation Measurements, 34: 415–418.
[20] Khatir, S.A., El-Ganawi, A.A., Ahmed, M.O., El-Khaangi, F.A., 1998. *Distribution of some natural and anthropogenic radionuclides in Sudanese harbour sediments*. Journal of Radioanalytical and Nuclear Chemistry, 237: 103–107.
[21] Khayrat, A.H., Oliver, M.A., Durrani, S.A., 2001. *The effect of soil particle size on soil radon concentration.* Radiation Measurements, 34: 365–371.
[22] Matiullah, A., Ur-Rehman, Sh., Ur-Rehman, A., Faheem, M., 2004. *Measurement of radioactivity in the soil of Behawalpur division, Pakistan*. Radiation Protection Dosimetry, 112: 443–447.
[23] Nelson, M.S., Rittenour, T.M., 2015. *Using grain-size characteristics to model soil water content: Application to dose-rate calculation for luminescence dating*. Radiation Measurements, 81: 142–149.
[24] Ramli, A.T., Wahab, A., Hussein, M.A., Wood, A.K., 2005. *Environmental ^{238}U and ^{232}Th concentration measurements in an area of high level natural background radiation at Palong, Johor, Malaysia*. Journal of Environmental Radioactivity, 80: 287–304.
[25] Rasas, M.F., Yassin, S.S., Shabat, M.M., 2004. *Measurements of the radon-222 and its daughter's concentrations throughout Gaza Strip, Palestine*. Proceeding of the Environmental Physics Conference, 24–28 February, Egypt.
[26] Schubert, M., Peña, P., Balcázar, M., Meissner, R., Lopez, A., Flores, J.H., 2005 . *Determination of radon distribution patterns in the upper soil as a tool for the localization of subsurface NAPL contamination*. Radiation Measurements, 40: 633–637.
[27] Shafi-ur-Rehman, Matiullah, Shakeel-ur-Rehman, Rahman, S., 2006. *Studying ^{222}Rn exhalation rate from soil and sand samples using CR-39 detector*. Radiation Measurements, 41: 708–713.
[28] Shweikani, R., Giaddui, T.G., Durrani, S.A., 1995. *The effect of soil parameters on the radon concentration values in the environment*. Radiation Measurements, 25: 581–584.
[29] Sroor, A., El-Bahi, S.M., Ahmed, F., Abdel-Haleem, A.S., 2001. *Natural radioactivity and radon exhalation rate of soil in southern Egypt*. Applied Radiation and Isotopes, 55: 873–879.
[30] Tzortzis, M., Tsertos, H., Christofides, S., Christodoulides, G., 2003. *Gamma-ray measurements of naturally occurring radioactive samples from Cyprus characteristic geological rocks*. Radiation Measurements, 37: 221–229.
[31] Ubeid, K.F., 2010. *Marine lithofacies and depositional zones analysis along coastal ridges in Gaza Strip, Palestine*. Journal of Geography and Geology, 2: 68–76.
[32] Ubeid, K.F., 2011. *The nature of the Pleistocene-Holocene palaeosols in the Gaza Strip, Palestine*. Geologos, 17: 163–173.
[33] Ubeid, K.F., 2013. *The origin, nature and stratigraphy of Pleistocene-Holocene palaeosols in Wadi Es-Salqa (Gaza Strip, Palestine)*. Serie Correlación Geológica, 29: 63–78.
[34] Ubeid, K.F., Albatta, A., 2014. *Sand dunes of the Gaza Strip (southwestern Palestine): Morphology, textural characteristics and associated environmental impacts*. Earth Sciences Research Journal, 18: 131–142.
[35] Ubeid, K.F., Ramadan, K.A., 2017. *Activity concentration and spatial distribution of radon in beach sands of Gaza Strip, Palestine*. Journal of Mediterranean Earth Sciences, 9: 19–28.
[36] UNSCEAR, 2000. *Sources and Effects of Ionizing Radiation*. Report to General Assembly, with Scientific Annexes. UN, New York.
[37] Veiga, R., Sanches, N., Anjos, R., 2006. *Measurement of natural radioactivity in Brazilian beach sands*. Radiation Measurements, 41: 189–196.